Received: 1 June 2021 | Revised: 27 September 2021 | Accepted: 27 September 2021

DOI: 10.1111/mpp.13153

Molecular Plant Pathology WILEY

ORIGINAL ARTICLE

Different epitopes of *Ralstonia solanacearum* effector RipAW are recognized by two *Nicotiana* species and trigger immune responses

Yang Niu[1] | Shouyang Fu[1] | Gong Chen[1] | Huijuan Wang[1] | Yisa Wang[1] | JinXue Hu[1] | Xin Jin[1] | Mancang Zhang[1] | Mingxia Lu[1] | Yizhe He[1] | Dongdong Wang[2] | Yue Chen[1] | Yong Zhang[3,4] | Núria S. Coll[5] | Marc Valls[5,6] | Cuizhu Zhao[1] | Qin Chen[2] | Haibin Lu[1,7]

[1]State Key Laboratory of Crop Stress Biology for Arid Areas, College of Agronomy, Northwest A&F University, Yangling, China

[2]Shaanxi Key State Laboratory of Crop Heterosis, Northwest A&F University, Yangling, China

[3]College of Food Science and Engineering, Northwest A&F University, Yangling, China

[4]College of Resources and Environment, Southwest University, Chongqing, China

[5]Interdisciplinary Research Center for Agriculture Green Development in Yangtze River Basin, Southeast University, Chongqing, China

[6]Centre for Research in Agricultural Genomics, CSIC-IRTA-UAB-UB, Bellaterra, Catalonia, Spain

[7]Department of Genetics, University of Barcelona, Barcelona, Spain

Correspondence

Haibin Lu, State Key Laboratory of Crop Stress Biology for Arid Areas, College of Agronomy, Northwest A&F University, Yangling, Shaanxi 712100, China.
Email: luhaibin011@hotmail.com

Cuizhu Zhao, State Key Laboratory of Crop Stress Biology for Arid Areas, College of Agronomy, Northwest A&F University, Yangling, China.
Email: zhaocuizhu2002@163.com

Qin Chen, College of Food Science and Engineering, Northwest A&F University, Yangling, China.
Email: chenpeter2289@nwsuaf.edu.cn

Funding information

Shaanxi the Nature Science Basic Research Plan, Grant/Award Number: 2020JM-160; the Fundamental Research Fund for the Central Universities of China, Grant/Award Number: Z109021706; the Programme of Introducing Talents of Innovative Discipline to Universities (Project 111) from the State administration of Foreign Experts Affairs, Grant/Award Number: B18042; External Science and Technology Cooperation

Abstract

Diverse pathogen effectors convergently target conserved components in plant immunity guarded by intracellular nucleotide-binding domain leucine-rich repeat receptors (NLRs) and activate effector-triggered immunity (ETI), often causing cell death. Little is known of the differences underlying ETI in different plants triggered by the same effector. In this study, we demonstrated that effector RipAW triggers ETI on *Nicotiana benthamiana* and *Nicotiana tabacum*. Both the first 107 amino acids ($N_{1\text{-}107}$) and RipAW E3-ligase activity are required but not sufficient for triggering ETI on *N. benthamiana*. However, on *N. tabacum*, the $N_{1\text{-}107}$ fragment is essential and sufficient for inducing cell death. The first 60 amino acids of the protein are not essential for RipAW-triggered cell death on either *N. benthamiana* or *N. tabacum*. Furthermore, simultaneous mutation of both R75 and R78 disrupts RipAW-triggered ETI on *N. tabacum*, but not on *N. benthamiana*. In addition, *N. tabacum* recognizes more RipAW orthologs than *N. benthamiana*. These data showcase the commonalities and specificities of RipAW-activated ETI in two evolutionally related species, suggesting *Nicotiana* species have acquired different abilities to perceive RipAW and activate plant defences during plant–pathogen co-evolution.

Yang Niu, Shouyang Fu, Gong Chen, and Huijuan Wang contributed equally.

This is an open access article under the terms of the Creative Commons Attribution-NonCommercial-NoDerivs License, which permits use and distribution in any medium, provided the original work is properly cited, the use is non-commercial and no modifications or adaptations are made.
© 2021 The Authors. *Molecular Plant Pathology* published by British Society for Plant Pathology and John Wiley & Sons Ltd.

Program of Ningxia Academy of Agriculture and Forestry Sciences, Grant/Award Number: DW-X-2018012; the Start-up Funds of Northwest A&F University, Grant/Award Number: Z111021601; National Natural Science Foundation of China, Grant/Award Number: 31901573; the Special Research project from Shaanxi province, Grant/Award Number: F2020221001; the Key Research and Development plan of Ningxia Province, Grant/Award Number: 2021BEF02033

KEYWORDS

cell death, E3 ligase, effector, effector-triggered immunity, *Nicotiana*, *Ralstonia solanacearum*, RipAW

1 | INTRODUCTION

Through evolution, plants have acquired two layers of immunity that enable them to perceive pathogens and induce plant defences. In the first layer, pattern recognition receptors (PRRs) localized on the plasma membrane directly detect conserved microbe-associated molecular patterns (MAMPs), resulting in activation of pattern-triggered immunity (PTI) (Wan et al., 2019). In turn, pathogens use effector proteins, which are delivered into the plant cell cytoplasm, to perturb physiological processes and suppress PTI in order to thrive inside plant hosts. Plants have evolved intracellular resistance (R) proteins to directly or indirectly perceive effectors, triggering effector-triggered immunity (ETI) (Jones & Dangl, 2006). ETI is often accompanied with a hypersensitive response (HR), a local cell death at the pathogen entry site (Balint-Kurti, 2019). Most R proteins are nucleotide-binding domain leucine-rich repeat receptors (NLRs), whose activation and downstream signalling mechanisms are being intensively studied (Jubic et al., 2019; Zhou & Zhang, 2020).

Ralstonia solanacearum is a soilborne pathogen that causes destructive vascular bacterial wilt disease on plants. The pathogen infects more than 200 plant species, including potato, tomato, tobacco, and many ornamental plants (Genin & Denny, 2012). *R. solanacearum* is considered one of the most important plant bacterial pathogens worldwide due to its long persistence in the soil, unusually large host range, broad geographical distribution, and unavailable resistant crop varieties (Mansfield et al., 2012). The main virulence determinants of *R. solanacearum* are the type III secretion system (T3SS) and its translocated effector proteins. The genome of *R. solanacearum* is estimated to encode about 70 T3SS effectors (Genin & Denny, 2012). To date very few *R. solanacearum* effectors have been functionally characterized in planta (Landry et al., 2020). For example, AWR5 acts as an inhibitor of the target of rapamycin pathway and enhances plant sensitivity to *R. solanacearum* (Popa et al., 2016). Simultaneously knocking out seven RipG effector genes decreases *R. solanacearum* virulence on tomato and *Arabidopsis* (Angot et al., 2006). The effector PopP2 decreases the DNA affinity of defence-promoting WRKY transcription factors by acetylation, repressing plant defence in *Arabidopsis*. The RPS4/RRS1-R receptor pair mimics PopP2 substrates to capture PopP2 and activate plant defence (Le Roux et al., 2015; Sarris et al., 2015). Effector RipAY degrades glutathione in plant cells through its γ-glutamyl cyclotransferase (GGCT) activity, altering the intracellular redox environment and suppressing plant immune responses (Fujiwara et al., 2016; Mukaihara et al., 2016; Sang et al., 2018), and RipAC interrupts MAPK-mediated phosphorylation of SGT1 to suppress ETI (Yu et al., 2020). Some effectors, such as Brg11, RipAK, and RipI, hijack the metabolism to promote *R. solanacearum* growth in planta (Wang et al., 2021; Wu et al., 2019; Xian et al., 2020).

Protein modification by ubiquitin is one of the most important posttranslational modifications in eukaryotes. It modulates the stability, activity, and sublocalization of target proteins (Kerscher et al., 2006; Zheng & Shabek, 2017). Ubiquitination is accomplished by the sequential function of three enzymes: a ubiquitin-activating enzyme (E1), a ubiquitin-conjugating enzyme (E2), and a ubiquitin ligase (E3). E3 ligases catalyse the transfer of ubiquitin from an E2 to lysine residues of the target substrates. E3 ligases have been categorized into the REALLY NEW INTERESTING GENE (RING) family and HOMOLOGUES TO THE E6AP CARBOXYL TERMINUS (HECT) family. RING-type E3 ligases directly transfer ubiquitin from E2 to their substrates, whereas the HECT-type E3 ligases form a thioester-linked intermediate with ubiquitin before ubiquitin attaches to the substrate (Zheng & Shabek, 2017). Albeit ubiquitination does not exist in prokaryotes, effectors from many pathogens mimic E3 ligases to promote their virulence on hosts (Spallek et al., 2009). Examples include *Pseudomonas syringae* AvrPtoB, XopL from *Xanthomonas campestris*, and RipG7 effectors from *R. solanacearum*. AvrPtoB belongs to the RING E3 ligase family and suppresses Fen-mediated ETI on tomato and PRRs-mediated PTI in *Arabidopsis* by ubiquitinating and degrading Fen and PRRs through the 26S proteasome (Abramovitch et al., 2006; Gimenez-Ibanez et al., 2009; Gohre et al., 2008; Janjusevic et al., 2006). XopL acts as a RING-finger E3 ligase, whose E3 activity is required to eliminate stromules and induce plastid clustering (Erickson et al., 2018; Singer et al., 2013). RipG7 also harbours E3 ligase activity on still unknown substrates and plays a crucial role in pathogenicity on *Arabidopsis*, tomato, and *Medicago truncatula* (Angot et al., 2006). Recently, a conserved cysteine-dependent E3 ligase domain has been identified in animal and plant bacterial effectors such as SspH2 and SspH1 from *Salmonell*a, IpaH9.8 and IpaH3 from *Shigella*, and NopM from *Rhizobium*. They are named as the NEW E3 LIGASE (NEL) family because of their difference in both structure and mechanism from all known E3 ligases (Quezada et al., 2009; Singer et al., 2008; Xin et al., 2012; Zhu et al., 2008). RipAW from *R. solanacearum* RS1000 was reported to be a new member of the NEL family and to suppress PTI in *Nicotiana benthamiana*

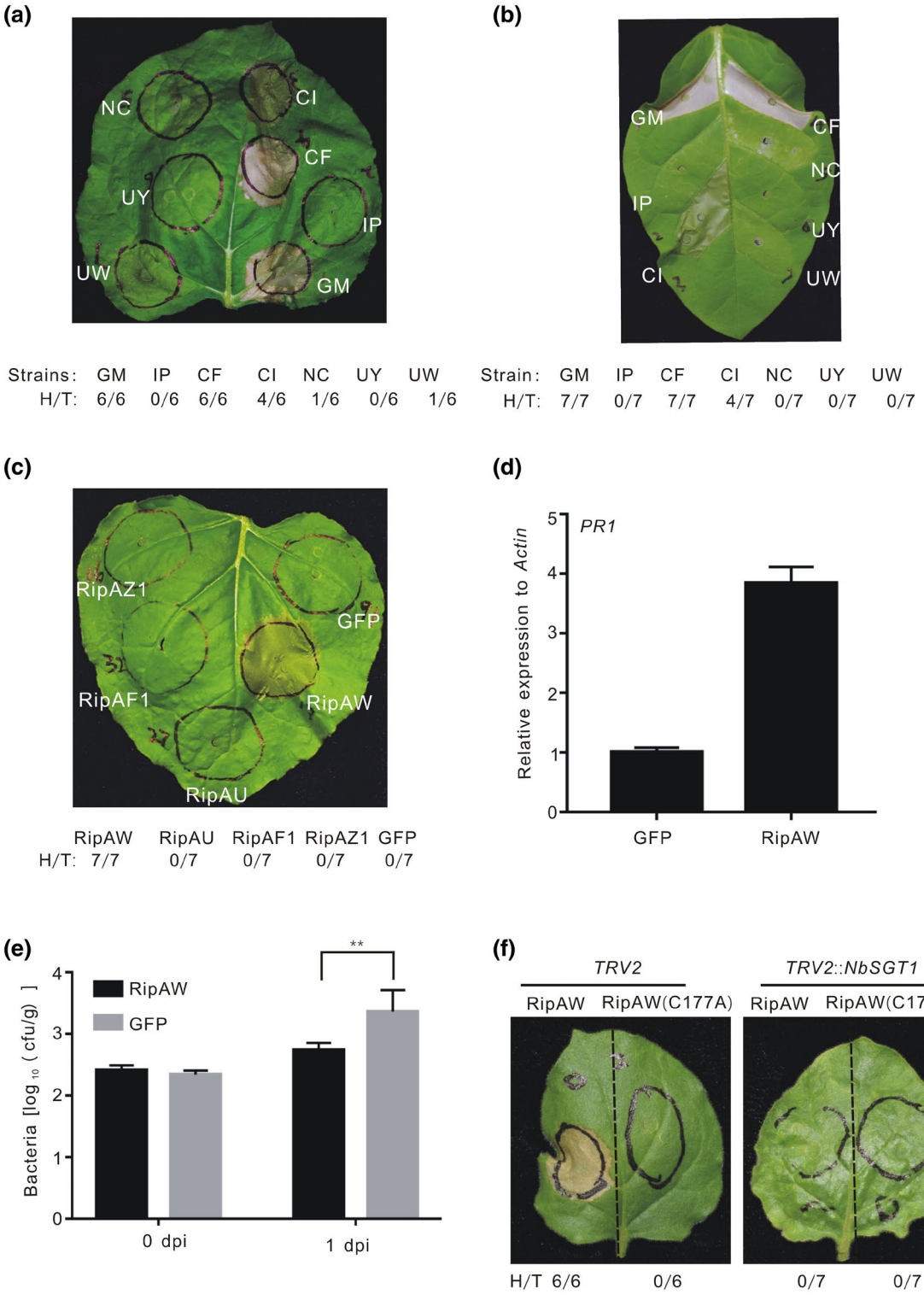

(Nakano et al., 2017). It has also been demonstrated that another *R. solanacearum* effector, RipV2, contains a NEL domain and plays a critical role in *R. solanacearum* infection on potato (Chen et al., 2021).

Species of *Nicotiana* are not only hosts for some *R. solanacearum* strains but also a very useful model to test gene function by the *Agrobacterium*-mediated transient expression assay. This transient expression system is widely used to study *R. solanacearum* effector function in hosts (Bally et al., 2018; Sabbagh et al., 2019). *R. solanacearum* effectors RipE1 and RipAW have been shown to subvert the flg22-triggered reactive oxygen species (ROS) burst, callose deposition, and defence-related gene expression on *N. benthamiana* (Jeon et al., 2020; Nakano & Mukaihara, 2019a; Nakano et al., 2017). Other effectors, such as RipB, RipE1, PopP1, and AvrA, are recognized by *Nicotiana* spp., leading to activation of ETI and cell death (Jeon et al., 2020; Nakano & Mukaihara, 2019b; Poueymiro et al., 2009; Sang et al., 2020; Sun et al., 2020; Zheng et al., 2019; Zhuo et al., 2020). Some

FIGURE 1 RipAW triggers cell death on *Nicotiana benthamiana*. Five-week-old *Nicotiana* spp. were leaf-inoculated with *Ralstonia solanacearum* strains or agrobacteria containing the effector constructs. (a, b) *R. solanacearum* strains GMI1000, CFBP2957, and CIP301 trigger cell death in *N. benthamiana* (a) and *Nicotiana tabacum* (b). Leaves inoculated with *R. solanacearum* strains were digitally photographed at 4 days postinoculation (dpi). (c) RipAW, but not RipAU, RipAF1, and RipAZ1, is able to trigger cell death in *N. benthamiana*. The photographs of leaves expressing those effectors were taken with a camera at 3 dpi. (d) Expression of RipAW enhances accumulation of *NbPR1*. The total RNA was extracted from the agroinfiltrated *N. benthamiana* leaves with RipAW and green fluorescent protein (GFP) control at 24 hours postinoculation (hpi). The expression of *NbPR-1* was determined by reverse transcription quantitative PCR and normalized to *NbActin*. (e) Expression of RipAW limits *R. solanacearum* JY1 growth. RipAW and control GFP were agroinfiltrated into *N. benthamiana* leaves. After 24 h, *R. solanacearum* JY1 strain solution (10^5 cfu) was infiltrated into the same leaves. Then the JY strain growth in leaves expressing *RipAW* was measured at the indicated times. Significant differences were evaluated with Student's *t* test (**$p < 0.01$). (f) NbSGT1 is required for RipAW-triggered cell death on *N. benthamiana*. The first two true leaves of 2-week-old *N. benthamiana* plants were infiltrated with agrobacteria carrying *TRV1*, *TRV2::NbSGT1*, *TRV2::GFP*, and *TRV2::NbPDS*. Then *NbSGT1*-silencing plants were agroinfiltrated with RipAW and investigated for RipAW-triggered cell death. The picture of RipAW-triggered cell death on *N. benthamiana* was taken at 5 dpi. All experiments were repeated three times with similar results. Strain names have been shortened in the image as follows: GMI1000 (GM), CFBP2957 (CF), CIP301 (CP), IPO1609 (IP), UW551 (UW), NCPPB3987 (NC), and UY031 (UY). H represents the number of leaves showing cell death, T represents the total number of *R. solanacearum* inoculated leaves

R. solanacearum effectors have acquired the ability to repress ETI. For example, RipAK targets catalases and inhibits their activities to abrogate *R. solanacearum*-triggered HR on *Nicotiana tabacum* 'Xanthi' (Sun et al., 2017) and RipAY degrades cellular glutathione to inhibit RipE1-triggered cell death on *N. benthamiana* (Sang et al., 2020).

Although several *R. solanacearum* effectors have been shown to trigger cell death in different *Nicotiana* species (Jeon et al., 2020; Landry et al., 2020), the molecular mechanism underlying this phenomenon has not been deeply investigated. In this study we describe that RipAW, a *R. solanacearum* GMI1000 effector, uses different ways to trigger cell death in *N. benthamiana* and *N. tabacum*, suggesting that different strategies have evolved in a single plant genus to detect the same pathogen effector.

2 | RESULTS

2.1 | Cell death on *N. benthamiana* caused by the effector RipAW is NbSGT1-dependent

R. solanacearum GMI1000 (phylotype I) triggers a very strong HR on *N. benthamiana* and *N. tabacum*, while the distantly related strain UW551 (phylotype II) does not trigger this response (Poueymiro et al., 2009). To find out whether other phylotype II strains fail to trigger cell death in both *Nicotiana* species, bacterial solutions of strains CIP301 and CFBP2957 (phylotype IIA) and UY031, UW551, IPO1609, and NCPPB3987 (phylotype IIB) as well as the control GMI1000 were directly infiltrated into the leaves of *Nicotiana* spp. Strains GMI1000, CIP301, and CFBP2957, but not those belonging to phylotype IIB (UY031, UW551, IPO1609, and NCPPB3987) induced strong cell death in *N. benthamiana* and *N. tabacum* at 3 days postinoculation (dpi; Figure 1a,b). However, cell death trigged by CIP301 in both plants was weaker than that caused by GMI1000 and CFBP2957 (Figure 1a,b). A functional T3SS is required for cell death triggered by the strain GMI1000 on *Nicotiana* species (Poueymiro et al., 2009), implying that the observed cell death in Figure 1a could be attributed to the activity of an effector. Instead of analysing the natural variation of all known cell death-triggering effectors among strains (Jeon et al., 2020; Landry et al., 2020; Sang et al., 2020), we preferred to explore new cell death-triggering effectors. We guessed that the effectors might be conserved among cell death-triggering strains but absent from those strains unable to cause this response. Because the genomes of CIP301 and NCPPB3987 are not available on public databases, we searched which effectors were present in GMI1000 and CFBP2957 but absent in UW551 and UY031. Using the Ralsto T3E tool (www.ralsto-T3E.org) (Sabbagh et al., 2019), we identified only seven effectors that met this criterion: RipAW, RipAZ1, RipAU, RipAF1, RipA4, RipS4, and RipJ. To determine whether these effectors triggered cell death, RipAW, RipAZ1, RipAU, and RipAF1 from the strain GMI1000 and green fluorescent protein (GFP) as a control were transiently expressed in *N. benthamiana* by agroinfiltration. We found that RipAF1, RipAZ1, RipAU, or GFP did not trigger any visible cell death, but RipAW induced a very strong tissue collapse and ion leakage on *N. benthamiana* (Figures 1c and S1). This observation suggested that RipAW might contribute to GMI1000 and CFBP2957-induced cell death in *Nicotiana* spp.

To test whether cell death triggered by RipAW results from the activation of plant immune responses, we checked the expression of *PATHOGENESIS-RELATED 1* (*PR1*) on *N. benthamiana*, used as a marker gene of salicylic acid-mediated plant immunity (Ding & Ding, 2020). RipAW expression significantly increased the expression level of *NbPR1* compared with that of GFP (Figure 1d). To determine whether or not the immune response triggered by RipAW affects the proliferation of *R. solanacearum* in plants, we measured *R. solanacearum* JY1 growth on RipAW-expressing *N. benthamiana* leaves. Compared with GFP control, the expression of RipAW significantly restricted JY1 growth (Figure 1e). The expression of GFP and RipAW was detected by western blot (Figure S2). This suggests that RipAW can be recognized by *N. benthamiana*, activating plant immunity and cell death, which is a typical feature of ETI (Jones & Dangl, 2006). SGT1 plays a critical role in ETI signalling by regulating the stability of NLR proteins (Azevedo et al., 2002; Holt et al., 2005). To examine whether or not RipAW-triggered cell death is dependent on NbSGT1, we investigated RipAW-triggered cell death in *N. benthamiana* after knocking down *NbSGT1* by virus-induced gene silencing (VIGS). We found that the cell death triggered by RipAW was specifically abolished in *NbSGT1*-silenced plants, but not in control plants (Figures 1f

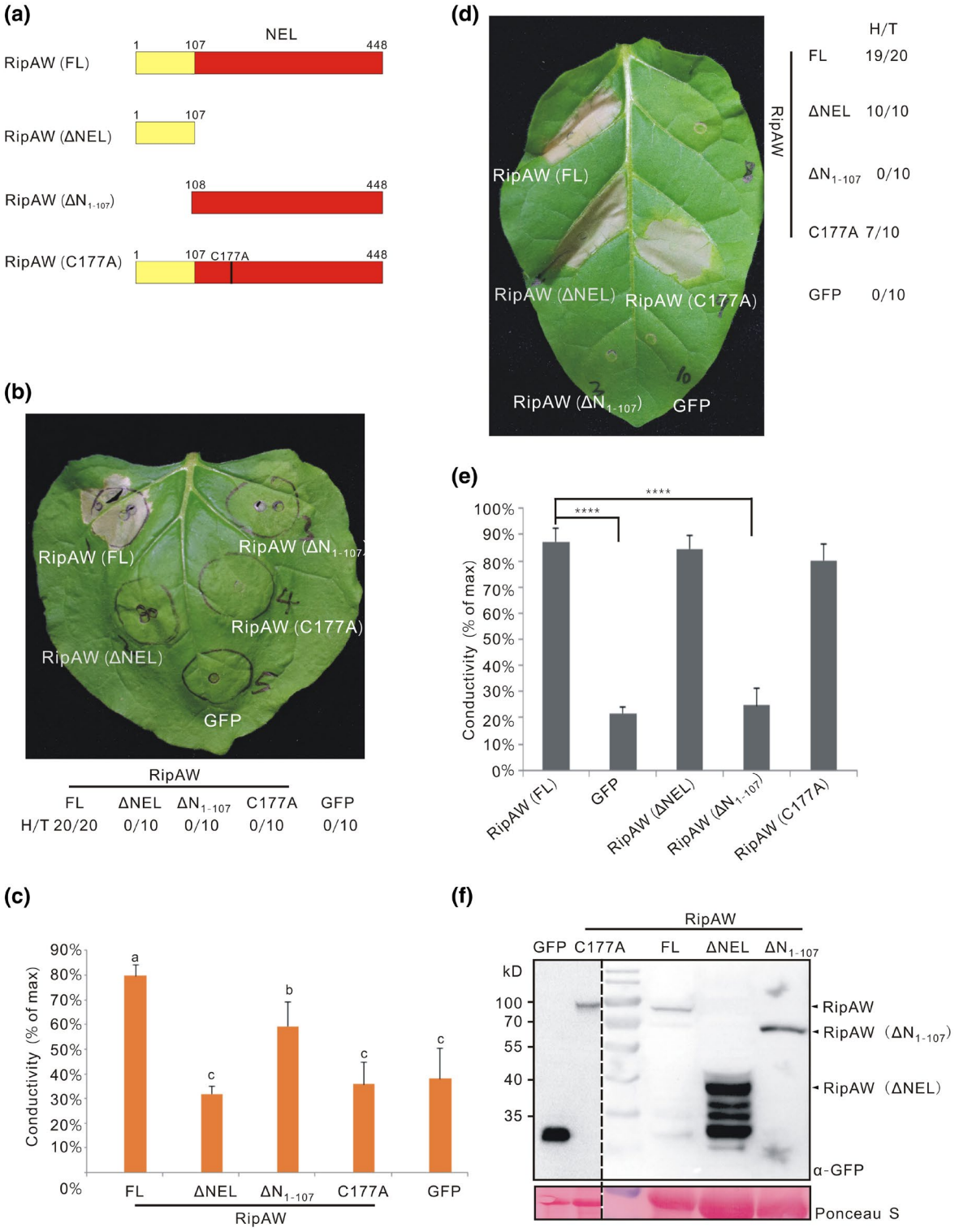

and S3). This suggests that RipAW might be perceived by (an) NLR receptor(s) eliciting ETI in *N. benthamiana*.

2.2 | E3 ligase activity is required, but not sufficient for RipAW-triggered cell death in *N. benthamiana*

RipAW from the strain GMI1000 ($RipAW_{GM}$) induced strong cell death (Figure 1), while a previous report showed that RipAW from strain RS1000 ($RipAW_{RS}$) induced leaf chlorosis on *N. benthamiana* instead of cell death, and that this phenotype was dependent on its E3 ligase activity (Nakano et al., 2017). We decided to test whether $RipAW_{GM}$-triggered cell death was caused by a loss of its ligase activity. Recombinant glutathione S-transferase (GST)-tagged $RipAW_{GM}$ purified from *Escherichia coli* was directly incubated with human E1, human UbcH5B (E2), and the substrate HA-Ubiquitin in vitro, and the reaction mixture was subjected to western blot. A poly-ubiquitin ladder was detected with anti-HA antibody (Figure S4) indicating that

FIGURE 2 E3 ligase activity is essential for RipAW-triggered cell death in *Nicotiana benthamiana*, but not in *Nicotiana tabacum*. RipAW and its derivatives were transiently expressed in leaves of 5-week-old *Nicotiana* spp. by agroinfiltration. (a) Schematic illustration of RipAW and its derivatives RipAW (ΔNEL), RipAW ($\Delta N_{1\text{-}107}$), and RipAW (C177A). (b) Loss of E3 ligase activity abolishes RipAW-triggered cell death in *N. benthamiana*. Cell death phenotype on *N. benthamiana* was photographed at 4 days postinoculation (dpi) with a digital camera. (c) Cell death in (b) was quantified by investigating electrolyte leakage. The *N. benthamiana* leaves expressing RipAW and its derivatives were harvested at 4 dpi and the conductivity was measured by a conductimeter. Electrolyte leakage was manifested as the percentage of sample $\text{conductivity}_{\text{unboiling}}/\text{conductivity}_{\text{boiling}}$ (the following assay is similar). Different letters above the columns indicate significant differences between conditions (one-way analysis of variance, Tukey's test, $p < 0.01$). (d) E3 ligase activity is not required for RipAW-triggered cell death in *N. tabacum*. Photographs of cell death in *N. tabacum* induced by RipAW and its mutants were taken at 4 dpi. (e) Cell death in (d) was quantified by measuring electrolyte leakage. The agroinfiltrated leaves were collected at 4 dpi and their electrolyte leakage was measured with a conductimeter. Asterisks indicate significant differences between RipAW mutants and RipAW (FL) (Student's *t* test, $^{****}p < 0.001$). (f) Detection of RipAW and its derivatives in *N. benthamiana* with western blot using anti-GFP antibody. Leaves expressing RipAW and its mutants were harvested and protein was extracted around 24 h after agroinfiltration. H is the number of leaves with cell death and T is the total number of infiltrated leaves. All experiments were repeated three times with the similar results

RipAW_{GM} is a functional E3 ligase. Importantly, the poly-ubiquitin ladder was completely abrogated when cysteine 177 was substituted by an alanine or a serine (Figure S4), suggesting that this is the key catalytic residue for RipAW E3 ligase activity, consistent with the NEL family features (Nakano et al., 2017; Quezada et al., 2009).

Subsequently, to understand whether the E3 ligase domain is sufficient for RipAW-triggered cell death, we split the full length RipAW into an N-terminal fragment spanning 1–107 residues [RipAW (ΔNEL)] and an NEL-domain containing fragment [RipAW ($\Delta N_{1\text{-}107}$)] (Figure 2a). Neither RipAW (ΔNEL) nor RipAW ($\Delta N_{1\text{-}107}$) caused leaf tissue collapse (Figure 2b). However, electrolyte leakage assay showed RipAW ($\Delta N_{1\text{-}107}$) induced higher conductivity than RipAW (ΔNEL) (Figure 2c). Western blot analysis with anti-GFP antibody confirmed the expression of RipAW and its variants in *N. benthamiana* (Figure 2f). These results indicate that both the N-terminus and the NEL domain are required for RipAW-triggered cell death in *N. benthamiana*. To explore the role of the E3 ligase activity in RipAW-triggered cell death in plants, we analysed cell death in *N. benthamiana* leaves expressing RipAW (C177A). In contrast to clear tissue collapse caused by RipAW, the C177A mutation completely abolished cell death symptoms (Figure 2b). We further quantified cell death by measuring ion leakage and found that the conductivity caused by RipAW (C177A) was comparable to the GFP control and clearly lower than that caused by RipAW (Figure 2c). These results indicate that the E3 ligase activity of RipAW is essential for cell death in *N. benthamiana*.

2.3 | The 107 N-terminal amino acid residues, not its E3 ligase activity, is required for RipAW- triggered cell death on *N. tabacum*

To test whether RipAW and its variants also trigger cell death in *N. tabacum*, we agroinfiltrated them and investigated cell death display in *N. tabacum*. When the full length of RipAW was expressed, a very clear cell death phenotype appeared compared to the GFP control, which is consistent with the cell death-inducing ability of the strain GMI1000 in *N. tabacum* (Figure 1b). Unexpectedly, RipAW (ΔNEL), but not RipAW ($\Delta N_{1\text{-}107}$), retained the ability to induce cell death in *N. tabacum* (Figure 2d,e), implying that the first 107 amino acids fragment ($N_{1\text{-}107}$) of RipAW are required and sufficient for eliciting cell death in *N. tabacum*. In line with this, the E3 ligase mutant RipAW (C177A) still kept the ability to induce cell death (Figure 2d,e). These results indicate that in contrast to *N. benthamiana*, the RipAW 107 N-terminal amino acids fragment, but not E3 ligase activity, is required for RipAW-triggered cell death in *N. tabacum*, suggesting that *N. tabacum* and *N. benthamiana* employ different strategies to initiate the cell death programme on RipAW recognition.

2.4 | The first 60 amino acids of RipAW are not required for the activation of cell death on *Nicotiana* spp.

The $N_{1\text{-}107}$ fragment is required for RipAW-triggered cell death in both *N. benthamiana* and *N. tabacum* (Figure 2). To further check the effect of the N-terminus on the function of RipAW on *Nicotiana* spp., we generated a series of truncated RipAW versions by deleting 30 amino acids from its N-terminus and investigated cell death by transiently expressing them in *N. benthamiana* (Figure 3a). Leaves infiltrated with RipAW ($\Delta N_{1\text{-}60}$) displayed strong cell death phenotypes, while those infiltrated with RipAW ($\Delta N_{1\text{-}30}$) and RipAW ($\Delta N_{1\text{-}90}$) looked healthy (Figure 3b). Consistent with the leaf symptoms, ion leakage assays showed that leaf conductivity triggered by RipAW ($\Delta N_{1\text{-}60}$) was indiscernable from that of RipAW, which was clearly higher than RipAW ($\Delta N_{1\text{-}30}$) and RipAW ($\Delta N_{1\text{-}90}$) (Figure 3c). Similar to *N. benthamiana*, deletion of these first 60 amino acids did not affect RipAW-triggered cell death in *N. tabacum*, but lack of the first 90 amino acids blocked cell death appearance (Figure 3d). Western blot analysis indicated that RipAW ($\Delta N_{1\text{-}30}$) was not expressed in *Nicotiana* spp., which may underpin the failure of RipAW ($\Delta N_{1\text{-}30}$) to elicit cell death (Figure 3e). Interestingly, all truncated proteins were detected as a single band, while the full-length RipAW showed two bands (Figure 3e).

2.5 | RipAW orthologs from different strains exhibit differential abilities to trigger cell death on *Nicotiana* species

RipAW is present in the genomes of 89 of the 155 sequenced *R. solanacearum* strains (Sabbagh et al., 2019). To explore if RipAWs from

different *R. solanacearum* strains have acquired the ability to subvert recognition by the immune surveillance system of *N. benthamiana*, we synthesized RipAW orthologs from representative strains in the four phylotypes: RS1000 (RS, phylotype I), CFBP2957 (CF, phylotype IIA), Po82 (Po, phylotype IIB), and CMR15 (CM, phylotype III) and PSI07 (PS, phylotype IV) (Sabbagh et al., 2019), and expressed these RipAW orthologs ($RipAW_{RS}$, $RipAW_{CM}$, $RipAW_{PS}$, $RipAW_{CF}$, and $RipAW_{Po}$) by agroinfiltration on *Nicotiana* spp. We found that $RipAW_{RS}$ induced clear cell death in leaves of *N. benthamiana*, while other RipAWs did not trigger this response (Figure 4a). Western blot analysis showed that $RipAW_{CM}$ and $RipAW_{PS}$ were undetectable, therefore they were excluded from subsequent assays (Figure 4c). Consistent with the observed macroscopic cell death, leaves expressing $RipAW_{CF}$ and $RipAW_{Po}$ showed significantly lower conductivities than those expressing $RipAW_{GM}$ and $RipAW_{RS}$ (Figure 4b). This indicates that $RipAW_{CF}$ and $RipAW_{Po}$ might escape perception by *N. benthamiana*. In contrast, when inoculated on *N. tabacum* leaves, $RipAW_{Po}$ caused a strong cell death phenotype (Figure 4d). This reinforces the idea that these two *Nicotiana* species have evolved different surveillance systems to recognize members of the RipAW family.

2.6 | N-terminus of RipAW orthologs show differential abilities to induce cell death in *N. tabacum*

The $N_{1\text{-}107}$ region is responsible for cell death induced by $RipAW_{GM}$ in *N. tabacum* (Figure 2). Therefore we speculated that natural variation on the N-termini of allelic RipAWs might enable the RipAW N-terminus to overcome the *N. tabacum* recognition system. Because $RipAW_{CM}$ and $RipAW_{PS}$ could not be detected by western blot (Figure 4), we investigated the role in cell death of $RipAW_{GM}$, $RipAW_{RS}$, $RipAW_{CF}$, and $RipAW_{Po}$ N-termini. We aligned the protein sequences of RipAW orthologs (Figure S5), identified and cloned their N-termini, and expressed them in *N. tabacum* by agroinfiltration. Both cell death symptoms and ion leakage assays showed that RipAW $(N_{1\text{-}107})_{GM}$, RipAW $(N_{1\text{-}107})_{RS}$, and RipAW$(N_{1\text{-}90})_{CF}$ elicited strong cell death and ion leakage in *N. tabacum* leaves while RipAW $(N_{1\text{-}90})_{Po}$ did not cause any cell death in *N. tabacum* (Figure 5a,b). These data suggest that although *N. tabacum* possesses a very powerful surveillance system to detect the divergent N-termini of RipAW orthologs and activate cell death, some *R. solanacearum* strains have acquired supposedly undetectable variations at RipAW N-termini as a strategy to overcome this surveillance system during the arms race between *R. solanacearum* and its plant hosts.

2.7 | N-terminal arginines R75 and R78 are required for $RipAW_{GM}$-triggered cell death in *N. tabacum*, but not in *N. benthamiana*

To explore how $RipAW_{CF}$ and $RipAW_{Po}$ escape *N. benthamina* detection, we analysed their protein sequences using Cluster Omega. Strikingly, in comparison to $RipAW_{GM}$ and $RipAW_{RS}$, $RipAW_{CF}$ and $RipAW_{Po}$ lacked a 17 amino acid fragment after position 61 (Figure S5). This raised the possibility that this N-terminal peptide may function in $RipAW_{GM}$-induced cell death on *N. benthamiana*. Because charged amino acids normally play very important roles in maintaining protein configurations and in protein–protein interactions, we generated two $RipAW_{GM}$ double point mutants, RipAW (H62D/H64D) and RipAW (R75A/R78A), by substituting two histidine and two arginine residues with aspartate and alanine, respectively, in this region. These mutated versions of RipAW were agroinfiltrated on *N. benthamiana* and cell death was investigated. While the H62D/H64D mutations did not affect cell death caused by RipAW, the expression of RipAW (R75A/R78A) resulted in patchy yellowing of the leaves, suggesting that the R75A and R78A mutations attenuate RipAW-triggered cell death in *N. benthamiana* (Figure 6a). However, quantification of cell death by ion leakage did not show significant differences between RipAW and RipAW (R75A/R78A), although the conductivity value triggered by RipAW (R75A/R78A) was slightly lower (Figure 6b). Both mutated variants of RipAW showed similar protein levels to the wild-type protein (Figure 6e). These results indicate that the arginine R75/R78 and histidine H62/H64 residues of RipAW have a negligible role in cell death elicited by this effector in *N. benthamiana*.

Considering that the N-terminal fragment (1–107) of RipAW is sufficient for triggering cell death in *N. tabacum*, we speculate that the R75A/R78A mutation might alter RipAW-triggered cell death in this species. To test this idea, the RipAW (R75A/R78A) and RipAW (H62D/H64D) were expressed in *N. tabacum* leaves. Similar to what we observed in *N. benthamiana*, the H62D/H64D mutation did not alter RipAW-triggered cell death in *N. tabacum*. Interestingly, the R75A/R78A mutation completely suppressed RipAW-elicited cell death (Figure 6c,d). These results suggest that in contrast to *N. benthamiana*, R75 and R78 play an important role in $RipAW_{GM}$-triggered cell death in *N. tabacum*. These data again imply that *N. tabacum* and *N. benthamiana* use different strategies to detect RipAW and initiate ETI.

2.8 | Loss of function RipAW does not change the virulence/avirulence of *R. solanacearum* on solanaceous plants

To determine the contribution of RipAW in GMI1000-triggered cell death, we generated a mutant strain in which the RipAW coding sequence was completely deleted from its genome (Δ*ripAW*), and investigated the effect of this mutation on cell death in *Nicotiana* spp. The Δ*ripAW* strain was able to trigger cell death in both *N. benthamiana* and *N. tabacum* to similar levels as the wild-type strain GMI1000 (Figure S6a). Consistent with cell death symptoms, no difference in conductivity was detected between the wild type strain and the Δ*ripAW* strain (Figure S6b), suggesting that GMI1000-triggered cell death was mediated by additional effectors besides RipAW. This result is consistent with previous findings demonstrating that RipB, AvrA, PopP1, and RipE1 effectors trigger cell death in *N. benthamiana* or *N. tabacum* (Jeon et al., 2020; Nakano & Mukaihara, 2019a, 2019b; Poueymiro et al., 2009; Sang et al., 2020).

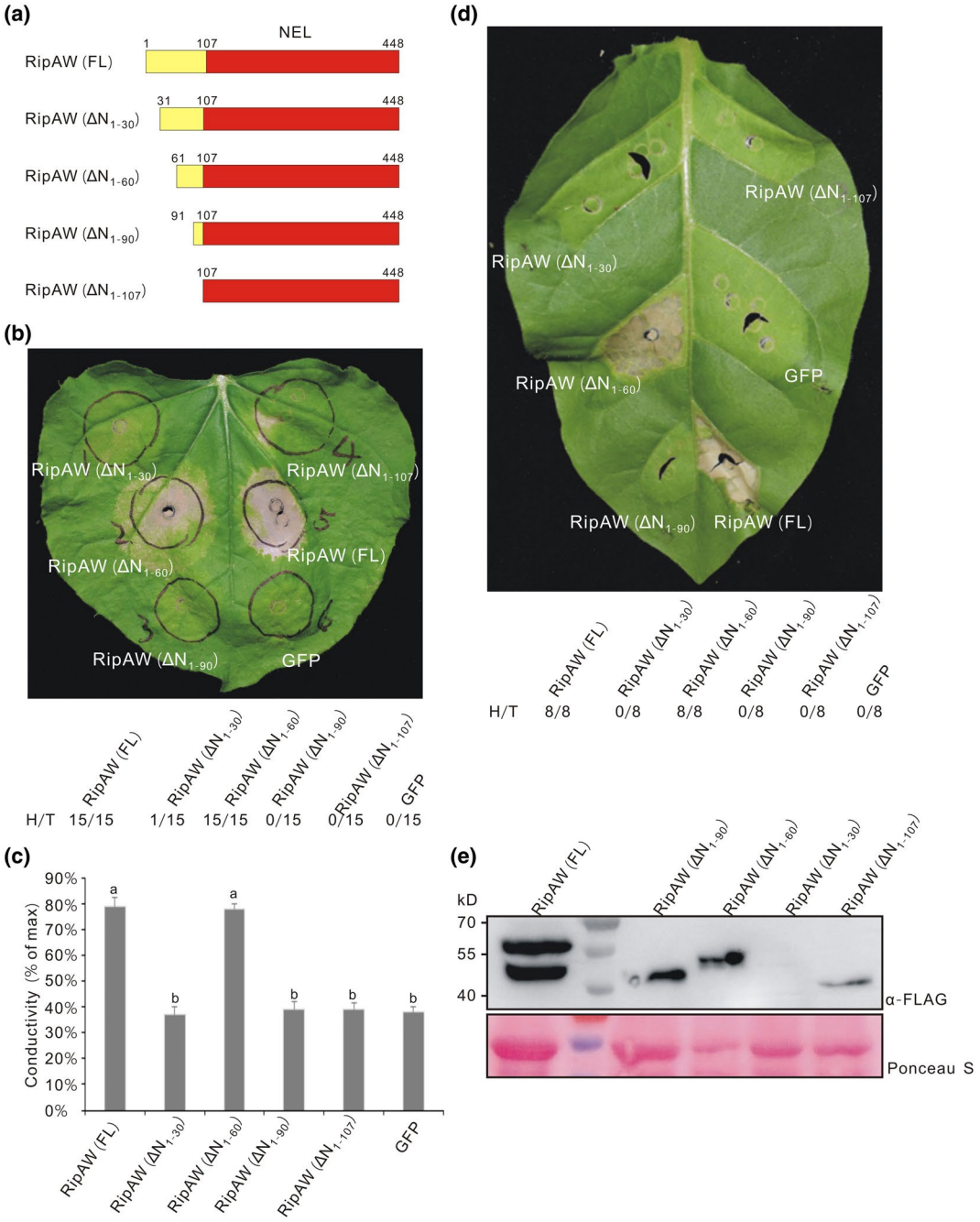

FIGURE 3 The first 60 N-terminal amino acids are not required for RipAW-triggered cell death on *Nicotiana* spp. RipAW N-terminal deletion mutants were agroinfiltrated into leaves of 5-week-old *N. benthamiana* and *N. tabacum*. (a) Schematic illustration of RipAW N-terminal mutants. (b) Deletion of the first 60 amino acids does not affect RipAW-triggered cell death on *N. benthamiana*. Leaves agroinfiltrated with RipAW mutants were digitally photographed at 4 days postinoculation (dpi). (c) Cell death triggered by the truncated RipAW variants in (b) was quantified by measuring ion leakage. *N. benthamiana* leaves expressing the truncated RipAW variants were collected at 4 dpi and immersed into double-deionized water. Then their ion leakage was measured with a conductimeter. Different letters above the columns indicate significant differences between conditions (one-way analysis of variance, Tukey's test, $p < 0.01$). (d) The first 60 amino acids are not essential for RipAW-triggered *N. tabacum* cell death. *N. tabacum* leaves agroinfiltrated with the truncated RipAW mutants were photographed at 5 dpi. (e) Detection of RipAW and its mutant variants in *N. benthamiana* with western blot using anti-FLAG antibody. The leaves expressing RipAW and its mutants were harvested and protein was extracted around 24 h after agroinfiltration. H is the number of leaves displaying cell death and T is the total number of infiltrated leaves. All experiments were repeated three times with similar results

Because *R. solanacearum* GMI1000 also causes brown rot disease on potato, we used an in vitro potato infection system to investigate whether this deletion affected the pathogen's fitness on potato plants (Wang et al., 2019). Similar to the wild-type strain, the mutant strain caused severe wilting symptoms on potato (Figure S6c,d). In line with this, *R. solanacearum* wild-type strain and Δ*ripAW* strain

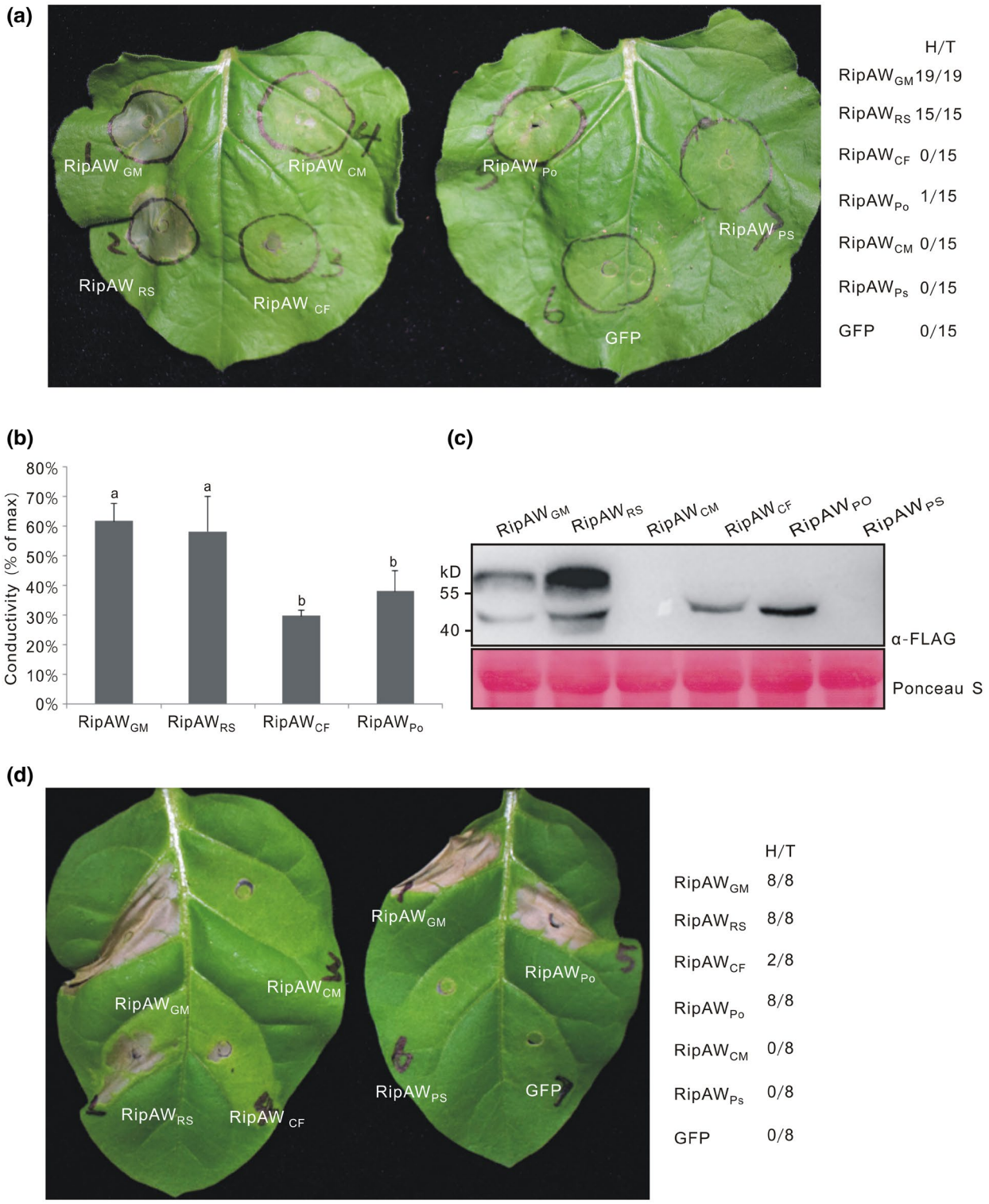

FIGURE 4 RipAW orthologs exhibit differential abilities to trigger cell death on *Nicotiana* spp. RipAW members from different strains were transiently expressed on leaves of 5-week-old *Nicotiana* spp. by agroinfiltration. (a) $RipAW_{RS}$ orthologs triggered strong cell death on *N. benthamiana*. Leaves expressing RipAW orthologs were photographed at 4 days postinoculation (dpi). (b) Cell death in (a) was quantified by measuring electrolyte leakage. The conductivities of *N. benthamiana* leaves agroinfiltrated with RipAW orthologs were measured with a conductimeter at 4 dpi. Different letters above columns indicate significant differences between conditions (one-way analysis of variance, Tukey's test, $p < 0.01$). (c) The expression of RipAW orthologs in *N. benthamiana* was detected by western blot using anti-FLAG antibody. Leaves expressing RipAW orthologs were harvested and protein was extracted at 24 h after agroinfiltration. (d) $RipAW_{RS}$ and $RipAW_{Po}$ triggered *N. tabacum* cell death. Leaves agroinfiltrated with RipAW family members were photographed at 5 dpi. H is the number of leaves with cell death and T is the total number of infiltrated leaves. The experiments were repeated three times with similar results

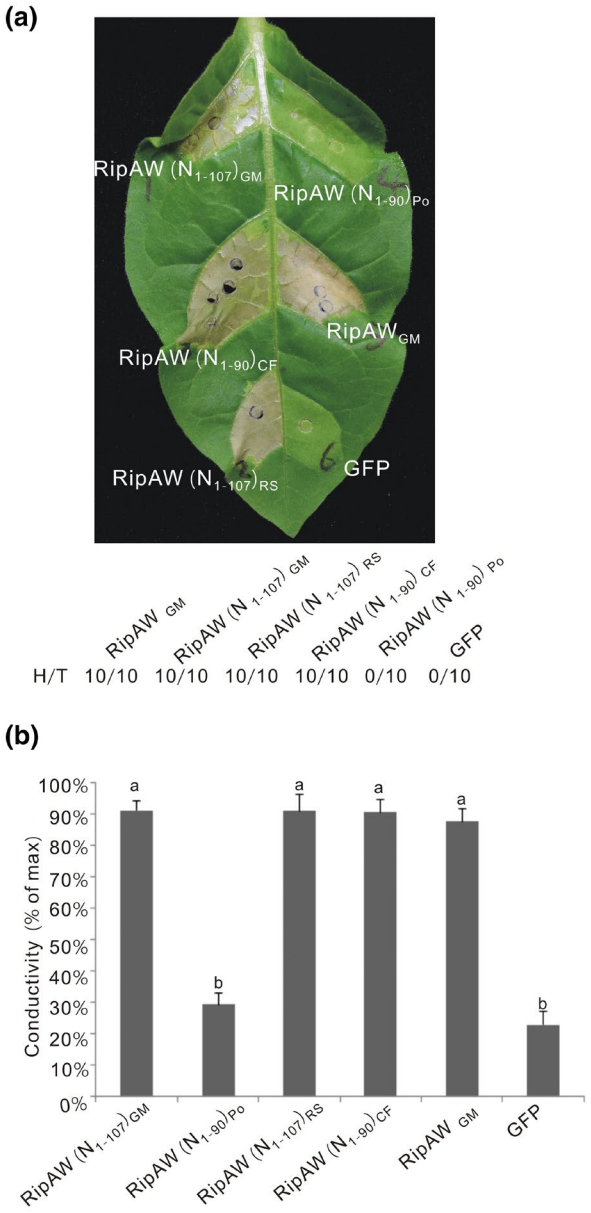

FIGURE 5 RipAW $(N_{1\text{-}90})_{CF}$ and RipAW $(N_{1\text{-}107})_{RS}$ induce strong cell death on *Nicotiana tabacum*. (a) Expression of RipAW $(N_{1\text{-}90})_{CF}$ and RipAW $(N_{1\text{-}107})_{RS}$ caused strong cell death. Leaves transiently expressing the N-terminus of RipAW orthologs were photographed at 4 days postinoculation (dpi). (b) Cell death in (a) was quantified by testing electrolyte leakage. Leaves agroinfiltrated with the N-terminus of RipAW orthologs were collected at 4 dpi and immersed in double-deionized water. Ion leakage was measured with a conductimeter. Different letters above the columns indicate significant differences between conditions (one-way analysis of variance, Tukey's test, $p < 0.01$). H is the number of dead leaves and T is the total number of infiltrated leaves. The experiments were repeated three times with similar results

reached similar growth levels in potato stems at 4 dpi, regardless of the inoculation method used (with or without wounding the roots) (Figure S6c,d). These results indicate that RipAW deficiency does not seem to affect the proliferation of *R. solanacearum* GMI1000 in potato plants.

3 | DISCUSSION

Effectors are the most important virulence determinants of gram-negative bacterial pathogens infecting plants. Occasionally, effectors betray the pathogen and activate ETI, resulting in failure of pathogen invasion. Except for a few examples, it remains largely unknown how different effectors together with different host targets induce ETI and cell death. Here, we characterized how $RipAW_{GM}$ from the bacterial wilt pathogen *R. solanacearum* triggered cell death in *Nicotiana* species (*N. benthamiana* and *N. tabacum*) in different ways. We found that the recognition of RipAW by *N. benthamiana* up-regulates defence-related gene *NbPR1* expression and activates cell death and plant immunity. Thus, the cell death triggered by RipAW is dependent on *NbSGT1*. We also showed that $RipAW_{RS}$ elicits very strong cell death in *N. benthamiana* and *N. tabacum* (Figure 4). However, Nakano and colleagues reported that $RipAW_{RS}$ induced leaf chlorosis, but not cell death in *N. benthamiana* (Nakano et al., 2017). This discrepancy could be attributed to the different experimental conditions used for plant growth (23°C and 70% humidity in our assay, 25°C and 50% humidity in Nakano's assay) and/or the *Agrobacterium* inoculum used for leaf infiltration (OD_{600} = 1 in our assay and OD_{600} = 0.5 in Nakano's assay).

The $RipAW_{GM}$ protein appears as two isoforms when expressed in *N. benthamiana* (Figures 3e and 6e). This could suggest that $RipAW_{GM}$ may undergo posttranslational modification(s) on its entry to the host cells. However, these two isoforms do not always have similar intensities (Figures S2 and 6e). Because the RipAW-FLAG size (471 amino acids) overlaps with that of the large subunit of RuBisCO, the observed two RipAW-FLAG bands might be artificial because the RuBisCO large subunit split one band into two, a phenomenon known as a "hamburger band". An alternative explanation is that RipAW undergoes proteolytic cleavage in planta. More experiments (such as immunoprecipitation assays) need to be performed to verify the nature of the two bands observed.

Deletion of RipAW did not have any noticeable effect on GMI1000-triggered HR on *Nicotiana* species (Figure S6a,b). This indicates that besides RipAW, other effectors also contribute to the cell death phenotype observed on *Nicotiana* species on infection. Consistent with this, several effectors, such as AvrA, PopP1, RipAB, RipB, RipE1, and RipI, have been sequentially shown to trigger cell death in *Nicotiana* species (Landry et al., 2020; Poueymiro et al., 2014). Interestingly, some *R. solanacearum* effectors suppress cell death triggered by other effectors in *Nicotiana*. For example, RipAY and RipAC block RipE1-induced *Nicotiana* leaf cell death by degrading glutathione and inhibiting SGT1-mediated MAPK activation (Sang et al., 2020; Yu et al., 2020). RipAK inhibits *R. solanacearum*-triggered cell death on *N. tabacum* (Sun et al., 2017). It will be interesting to know the inhibition spectrum of these effectors on the known *R. solanacearum* effector-triggered cell death. In potato, RipAW deficiency did not decrease GMI1000 pathogenicity (Figure S6c,d), similar to what has been previously shown in pepper and tomato (Nakano et al., 2017). Notably,

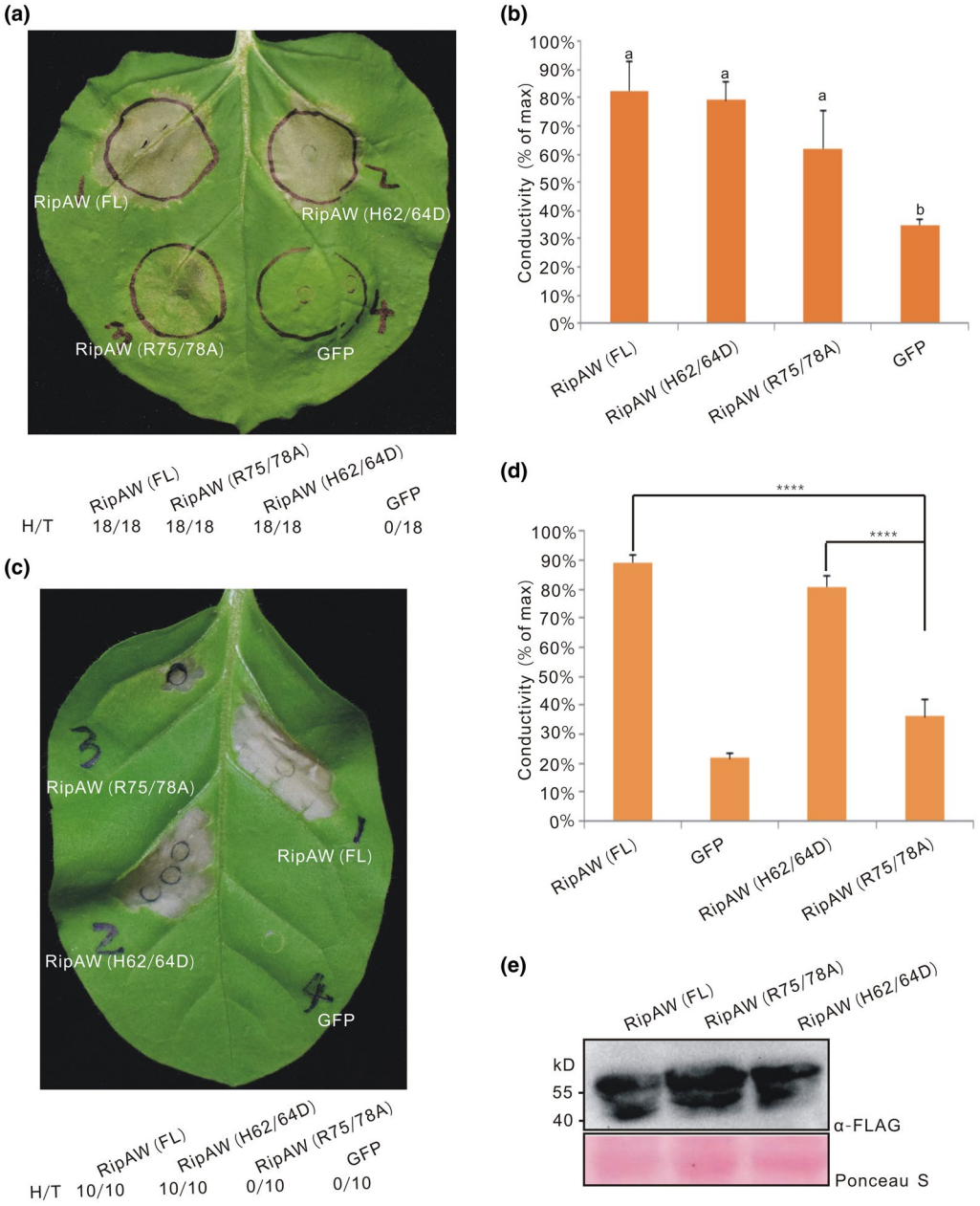

FIGURE 6 Arginine in positions 75 and 78 of RipAW is essential for cell death in *Nicotiana tabacum*. The indicated RipAW versions were agroinfiltrated into leaves of 5-week-old *Nicotiana* spp. (a) Substitution of both R75/R78 for alanine and H62/H64 for aspartate did not affect tissue collapse elicited by RipAW in *N. benthamiana*. Cell death symptoms on leaves expressing RipAW (R75/78A) and RipAW (H62/64D) were photographed at 4 days postinoculation (dpi). (b) Cell death induced by RipAW (R75/78A) and RipAW (H62/64D) on *N. benthamiana* was quantified by electrolyte leakage. Leaves expressing RipAW (R75/78A) and RipAW (H62/64D) were collected at 4 dpi and immersed in double-deionized water. The conductivity of samples was measured by a conductimeter. Different letters above columns indicate the significant difference (one-way analysis of variance, Tukey's test, $p < 0.01$). (c) Simultaneous mutation on R75 and R78 abolished cell death triggered by RipAW on *N. tabacum*. Cell death symptoms caused by RipAW (R75/78A) were photographed and the leaves showing cell death were counted at 4 dpi. (d) Cell death in (c) was quantified by electrolyte leakage assay. *N. tabacum* leaves agroinfiltrated with RipAW and its point mutants were harvested at 4 dpi and put into double-deionized water. Electrolyte leakage was detected by a conductimeter. Asterisks indicate statistically significant differences between RipAW and its variants (Student's *t* test, $^{****}p < 0.001$). (e) Expression of RipAW and its mutants was detected by western blot with anti-FLAG antibody in *N. benthamiana*. Leaves expressing RipAW point mutants were harvested and protein was extracted 24 h after agroinfiltration. H is the number of leaves with cell death and T is the total number of infiltrated leaves. The experiments were repeated three times with the similar results

overexpressing RipAW in *Arabidopsis* showed enhanced plant sensitivity to *P. syringae* DC3000, suggesting that RipAW inhibits plant immunity (Nakano et al., 2017). This implies that RipAW has functional redundancy with some of the 70 *R. solanacearum* effectors (Sabbagh et al., 2019). In agreement with this, lack of individual effectors in *P. syringae* does not change its virulence in terms of

bacterial growth in leaves and bacterial symptoms (Kvitko et al., 2009). In addition, restoration of most individual effectors to a DC3000 mutant strain lacking 28 effectors does not significantly enhance its virulence on plants (Cunnac et al., 2011). Similarly, disruption of single *R. solanacearum* effectors showed a very marginal effect on *R. solanacearum* virulence on plants (Cunnac et al., 2004; Sole et al., 2012). In addition, successful natural infection by *R. solanacearum* is a very complex process that has been divided into four steps: root colonization, vertical movements from roots to shoots, circular vascular bundle invasion, and radial apoplast spread in the cortex (Planas-Marques et al., 2020). Because wilting symptoms and large bacterial multiplication occur at late stages of *R. solanacearum* infection, we cannot exclude the possibility that RipAW plays a role in root colonization or bacterial movements inside the sensitive plant.

In this study, we proved the E3 ligase activity of $RipAW_{GM}$ is essential, but not sufficient for triggering cell death on *N. benthamiana* (Figure 2). On the contrary, the first 107 amino acids of RipAW are sufficient for cell death induction in *N. tabacum*, but not in *N. benthamiana* (Figure 2). Furthermore, mutation R72A/R78A blocks RipAW-triggered cell death in *N. tabacum*, but not in *N. benthamiana* (Figure 6). Together, these results indicate that *N. tabacum* and *N. benthamiana* employ different surveillance systems for sensing the effector RipAW and activating cell death and ETI. It will be very interesting to further explore how *N. benthamiana* and *N. tabacum* differentially perceive RipAW and activate ETI. Furthermore, although $RipAW_{Po}$ and $RipAW_{CF}$ escaped surveillance by the *N. benthamiana* immune system, they were still detected by *N. tabacum*. This suggests that the recognition spectrum of *N. tabacum* on RipAW might be broader than that of *N. benthamiana*. In the future, identifying the NLR proteins responsible for detecting RipAWs will help in deciphering the co-evolution strategies of NLR proteins and their cognate effectors during the long-lasting battle between host and pathogens. This will provide new insights into the molecular mechanism underlying recognition of allelic effectors by NLRs in different plant species during plant–microbe co-evolution and valuable information for breeding highly resistant crops based on NLR-protein mediated plant immunity.

4 | EXPERIMENTAL PROCEDURES

4.1 | Plant materials and microbial strains

Nicotiana spp. plants were sown in soil and grown in controlled chambers under 23°C and short-day conditions with 70% humidity. Potato explants of cv. Desirée were grown in liquid Murashige & Skoog medium with 20% sucrose (MS2) at 22–23°C, 70% humidity, and long-day conditions.

R. solanacearum strains GMI1000, CIP301, CFBP2957, UW551, IPO1905, NCPPB3987, and UY031 are described in Lu et al. (2018). Wild-type *R. solanacearum* JY1 strain was isolated from wilting tobacco plants (Yunyan 87) at Jiangyong county, Hunan province, China. The wild-type JY1 strain was transformed with a pHM1 plasmid which confers the ability of JY1 to grow on the spectinomycin-amended medium. All strains used in this study were grown at 28°C on solid or liquid rich B medium (1% Bacto peptone, 0.1% yeast extract, and 0.1% casamino acids; Becton Dickinson) with the appropriate antibiotics.

4.2 | Plasmid constructions

All primers used in this study are listed in Table S1. Genomic DNA of *R. solanacearum* GMI1000 was used as the template for PCR amplification of RipAW and its derivatives, which were cloned into pCambia 6604-GFP (*Bam*HI and *Sal*I/*Xho*I) (Bai et al., 2016) or pCambia1300-FLAG (*Kpn*I/*Sac*I and *Bst*BI) with a NovoRes plus one-step cloning kit (Novoprotein Scientific Inc.). The RipAW orthologs from strains RS1000, CFBP2957, PSI07, and Po82 were synthesized and cloned into pUC57 by the Gene Create company in Wuhan, China. These constructs were then directly digested with *Kpn*I and *Bst*BI and subcloned into pCambia 1300-FLAG with *Kpn*I and *Bst*BI. All plasmids made in this study are listed in Table S2.

4.3 | Construction of Δ*RipAW* strain

A 539 bp fragment at the upstream of RipAW start codon and a 682 bp fragment downstream of the RipAW stop codon were amplified from genomic DNA of *R. solanacearum* GMI1000 by chimeric PCR and were cloned into pURF80 vector. The resulting construct was introduced into *R. solanacearum* GMI1000 by natural transformation (Valls et al., 2006). The colonies grown on B medium containing 50 μg/ml kanamycin were selected and cultured in liquid B medium without antibiotics overnight. Cell cultures were spread on solid B medium containing 5% sucrose. Positive Δ*RipAW* candidates were confirmed by PCR.

4.4 | Ubiquitination assay

R. solanacearum GMI1000 RipAW was cloned into pGEX6p-1 vector with *Bam*HI/*Xho*I. PCR-based site-directed mutagenesis was used to mutate the cysteine 177 of RipAW into an alanine or a serine. The obtained pGEX-RipAW, pGEX-RipAW (C177A) and pGEX-RipAW (C177S) were transformed into *E. coli* BL21. The GST-tagged RipAW, RipAW (C177A), and RipAW (C177S) were purified from the IPTG-induced cell cultures by glutathione resin beads (Sigma) and detected by western blot with anti-GST antibody (Sigma).

Two micrograms of purified GST-tagged RipAW and its derivatives were incubated with 0.5 μg human E1, 2 μg UbcH5B E2, and 2 μg HA-ubiquitin (Boston Biochem) in 40 μl of reaction buffer (25 mM Tris.HCl pH 7.5, 50 mM NaCl, 5 mM ATP, 10 mM $MgCl_2$, 0.1 mM dithiothreitol) for 2 h at 37°C. The reaction was stopped by addition of 5× SDS-loading buffer. The reaction mixtures were separated by SDS-PAGE and detected with anti-GST antibody and anti-HA antibody (Sigma).

4.5 | *Agrobacterium*-mediated transient expression assay

Gene transient expression in *Nicotiana* species was performed as previously reported (Grosse-Holz et al., 2018). *Agrobacterium tumefaciens* GV3101 carrying RipAW and its derivatives were cultured in liquid LB medium at 28°C overnight, then collected by centrifugation and suspended with the inoculation buffer (10 mM MES pH 5.0, 10 mM $MgCl_2$, 400 nM acetosyringone). Five-week-old *N. benthamiana* and *N. tabacum* were infiltrated with *Agrobacterium* at an optical density of 1 (OD_{600} = 1) and covered with a transparent plastic membrane for 2 days and kept in a chamber under 23°C and long-day conditions with 70% humidity for gene expression.

4.6 | Cell death and ion leakage assay

To visualize cell death triggered by RipAW and its mutants on leaves, photographs of the leaves of *N. benthamiana* and *N. tabacum* inoculated with agrobacteria were taken with a digital camera at 4–5 dpi. For electrolyte leakage measurements, 15 leaf discs per sample were harvested, put into three tubes containing 5 ml of double-deionized water (five leaf discs/tuber), and subjected to vacuum for 20 min (Szczesny et al., 2010). Then all samples were left at room temperature for 2 h and the ion leakage caused by RipAW and its derivatives was measured with a conductimeter. To determine total conductivity of the entire sample, conductivity was measured again after boiling the solution for 20 min (Szczesny et al., 2010). Quantification of cell death triggered by RipAW and its mutants was displayed as the percentage of $Conductivity_{unboiling}$/$Conductivity_{boiling}$.

4.7 | Virus-induced gene silencing assay

An equal volume mixture of *Agrobacterium* (OD_{600} = 1) containing *TRV2::NbSGT1*, *TRV2::GFP*, and *TRV2::NbPDS* with *Agrobacterium* (OD_{600} = 1) carrying *TRV1* was infiltrated into the first two true leaves of 2-week-old *N. benthamiana*, which were then covered in plastic film for 2 days to keep high humidity. After that, the inoculated plants continued growing under 23°C and short-day conditions with 70% humidity for another 3 weeks. When plants inoculated with *TRV2::NbPDS* turned completely white (Senthil-Kumar et al., 2007), *TRV2::GFP* and *TRV2::NbSGT1* gene-silenced plants were agroinfiltrated with *RipAW* and its derivatives. After 3–4 dpi cell death phenotypes were investigated.

4.8 | *R. solanacearum* infection assay

R. solanacearum strains were grown at 28°C in liquid rich B medium overnight. Bacteria were collected by centrifugation and washed with sterile double-deionized water and adjusted to a final OD_{600} = 0.01. Five- to 6-week-old *N. benthamiana* plants were directly infiltrated with the bacterial solution. The inoculated *N. benthamiana* plants were put back into the infection chamber at 26°C, 75% humidity, and a 16 h light and 8 h dark photoperiod. Cell death symptoms were recorded at 3 dpi with a digital camera and quantified with electrolyte leakage (described above).

For potato explants infection we followed the protocol as described in Wang et al. (2019). Briefly, the roots of 2- to 3-week-old potato plants grown in liquid MS2 medium were cut with scissors and plants were subsequently transferred into glass jars containing 40 ml of a solution of *R. solanacearum* (OD_{600} = 0.01) and kept in the infection chamber under 26°C, 75% humidity, and 16 h light and 8 h dark photoperiod conditions. Photographs were taken with a digital camera and bacterial loads in the aerial part of the infected plants were measured when plants started wilting (Wang et al., 2019).

To measure *R. solanacearum* growth in *N. benthamiana*, we followed a *R. solanacearum* infection protocol (Sang et al., 2020) with minor modifications. Briefly, leaves were first infiltrated with agrobacteria containing RipAW (OD_{600} = 0.01), which is resistant to kanamycin. Around 20 h after agroinfiltration, a 10^5 cfu/ml solution of *R. solanacearum* JY1 with resistance to spectinomycin was inoculated by infiltration into the leaves expressing RipAW. *R. solanacearum* JY1 was isolated from wilting tobacco plants (Yunyan 87) at Jiangyong county, Hunan province, China and is also pathogenic on *N. benthamiana* (unpublished data). Twelve leaf discs were collected, weighed, and homogenized in sterile double-deionized water. Bacterial cfu were counted after plating on B medium with spectinomycin.

4.9 | Gene expression assay

Total RNA from leaves of *N. benthamiana* at the indicated times were extracted with TRIzol reagent (Invitrogen) and the first-strand cDNA was synthesized with an EvoM-MLV RT kit (Accurate Biotechnology). Five microlitres of the 20-fold diluted cDNA and primers (Table S1) was directly added into the SYBR Green Mix (Gene Star Co.). The prepared quantitative PCR (qPCR) solutions were run on a iQ7 real-time cycler (Life Technologies). Gene expression was quantified and normalized to *NbActin* using the $2^{-\Delta\Delta Ct}$ method.

4.10 | Statistical analysis

Statistical analyses were performed using Graphpad Prism v. 7.0 software. All statistical tests are indicated in the respective figure legends.

ACKNOWLEDGEMENTS

We are grateful to Dr Yu Du (Northwest A&F University) for the constructs *TRV1*, *TRV2::GFP*, *TRV2::NbSGT1*, and *TRV2::NbPDS*, and to Dr Changgen Xie for pCambia6604-GFP vector and Dr Wu Chen

(College of Plant Protection, Hunan Agricultural University) for *R. solanacearum* JY1. We also thank the Crop Biology Innovation Platform in the Agronomy College and Public Platform in the State Key Laboratory of Crop Stress Biology for Arid Areas at Northwest A&F University, China. This work was funded by the Nature Science Basic Research Plan of Shaanxi Province (2020JM-160), the Special Research project from Shaanxi province (F2020221001), the Program of Introducing Talents of Innovative Discipline to Universities (Project 111) from the State administration of Foreign Experts Affairs (B18042) and the External Science and Technology Cooperation Program of Ningxia Academy of Agriculture and Forestry Sciences (DW-X-2018012), the Start-up Funds of Northwest A&F University (Z111021601), the Fundamental Research Fund for the Central Universities of China (Z109021706), the Key Research and Development plan of Ningxia Province (2021BEF02033), and the National Natural Science Foundation of China for C.Z. (31901573).

DATA AVAILABILITY STATEMENT

All data supporting the findings of this study are available from the corresponding author upon reasonable request.

ORCID

Yong Zhang https://orcid.org/0000-0003-1820-0927
Marc Valls https://orcid.org/0000-0003-2312-0091
Haibin Lu https://orcid.org/0000-0002-0613-4697

REFERENCES

Abramovitch, R.B., Janjusevic, R., Stebbins, C.E. & Martin, G.B. (2006) Type III effector AvrPtoB requires intrinsic E3 ubiquitin ligase activity to suppress plant cell death and immunity. *Proceedings of the National Academy of Sciences USA*, 103, 2851–2856.

Angot, A., Peeters, N., Lechner, E., Vailleau, F., Baud, C., Gentzbittel, L. et al. (2006) *Ralstonia solanacearum* requires F-box-like domain-containing type III effectors to promote disease on several host plants. *Proceedings of the National Academy of Sciences USA*, 103, 14620–14625.

Azevedo, C., Sadanandom, A., Kitagawa, K., Freialdenhoven, A., Shirasu, K. & Schulze-Lefert, P. (2002) The RAR1 interactor SGT1, an essential component of R gene-triggered disease resistance. *Science*, 295, 2073–2076.

Bai, Y., Zhu, W., Hu, X., Sun, C., Li, Y., Wang, D. et al. (2016) Genome-wide analysis of the bZIP gene family identifies two ABI5-like bZIP transcription factors, BrABI5a and BrABI5b, as positive modulators of ABA signalling in Chinese cabbage. *PLoS One*, 11, e0158966.

Balint-Kurti, P. (2019) The plant hypersensitive response: concepts, control and consequences. *Molecular Plant Pathology*, 20, 1163–1178.

Bally, J., Jung, H., Mortimer, C., Naim, F., Philips, J.G., Hellens, R. et al. (2018) The rise and rise of *Nicotiana benthamiana*: a plant for all reasons. *Annual Review of Phytopathology*, 56, 405–426.

Chen, D., Zhou, D., Wang, Y., Wang, B., He, Q., Song, B. et al. (2021) *Ralstonia solanacearum* type III effector RipV2 encoding a novel E3 ubiquitin ligase (NEL) is requried for full virulence by suppressing plant PAMP-triggered immunity. *Biochemical and Biophysical Research Communication*, 550, 120–126.

Cunnac, S., Chakravarthy, S., Kvitko, B.H., Russell, A.B., Martin, G.B. & Collmer, A. (2011) Genetic disassembly and combinatorial reassembly identify a minimal functional repertoire of type III effectors in *Pseudomonas syringae*. *Proceedings of the National Academy of Sciences USA*, 108, 2975–2980.

Cunnac, S., Occhialini, A., Barberis, P., Boucher, C. & Genin, S. (2004) Inventory and functional analysis of the large Hrp regulon in *Ralstonia solanacearum*: identification of novel effector proteins translocated to plant host cells through the type III secretion system. *Molecular Microbiology*, 53, 115–128.

Ding, P. & Ding, Y. (2020) Stories of salicylic acid: a plant defense hormone. *Trends in Plant Science*, 25, 549–565.

Erickson, J.L., Adlung, N., Lampe, C., Bonas, U. & Schattat, M.H. (2018) The *Xanthomonas* effector XopL uncovers the role of microtubules in stromule extension and dynamics in *Nicotiana benthamiana*. *The Plant Journal*, 93, 856–870.

Fujiwara, S., Kawazoe, T., Ohnishi, K., Kitagawa, T., Popa, C., Valls, M. et al. (2016) RipAY, a plant pathogen effector protein, exhibits robust γ-γ-glutamyl cyclotransferase activity when stimulated by eukaryotic thioredoxins. *Journal of Biological Chemistry*, 291, 6813–6830.

Genin, S. & Denny, T.P. (2012) Pathogenomics of the *Ralstonia solanacearum* species complex. *Annual Review of Phytopathology*, 50, 67–89.

Gimenez-Ibanez, S., Hann, D.R., Ntoukakis, V., Petutschnig, E., Lipka, V. & Rathjen, J.P. (2009) AvrPtoB targets the LysM receptor kinase CERK1 to promote bacterial virulence on plants. *Current Biology*, 19, 423–429.

Göhre, V., Spallek, T., Häweker, H., Mersmann, S., Mentzel, T., Boller, T. et al. (2008) Plant pattern-recognition receptor FLS2 is directed for degradation by the bacterial ubiquitin ligase AvrPtoB. *Current Biology*, 18, 1824–1832.

Grosse-Holz, F., Madeira, L., Zahid, M.A., Songer, M., Kourelis, J., Fesenko, M. et al. (2018) Three unrelated protease inhibitors enhance accumulation of pharmaceutical recombinant proteins in *Nicotiana benthamiana*. *Plant Biotechnology Journal*, 16, 1797–1810.

Holt, B.F., Belkhadir, Y. & Dangl, J.L. (2005) Antagonistic control of disease resistance protein stability in the plant immune system. *Science*, 309, 929–932.

Janjusevic, R., Abramovitch, R.B., Martin, G.B. & Stebbins, C.E. (2006) A bacterial inhibitor of host programmed cell death defenses is an E3 ubiquitin ligase. *Science*, 311, 222–226.

Jeon, H., Kim, W., Kim, B., Lee, S., Jayaraman, J., Jung, G. et al. (2020) *Ralstonia solanacearum* type III effectors with predicted nuclear localization signal localize to various cell compartments and modulate immune responses in *Nicotiana* spp. *The Plant Pathology Journal*, 36, 43–53.

Jones, J.D.G. & Dangl, J.L. (2006) The plant immune system. *Nature*, 444, 323–329.

Jubic, L.M., Saile, S., Furzer, O.J., El Kasmi, F. & Dangl, J.L. (2019) Help wanted: helper NLRs and plant immune responses. *Current Opinion in Plant Biology*, 50, 82–94.

Kerscher, O., Felberbaum, R. & Hochstrasser, M. (2006) Modification of proteins by ubiquitin and ubiquitin-like proteins. *Annual Review of Cell and Developmental Biology*, 22, 159–180.

Kvitko, B.H., Park, D.H., Velasquez, A.C., Wei, C.F., Russell, A.B., Martin, G.B. et al. (2009) Deletions in the repertoire of *Pseudomonas syringae* pv. *tomato* DC3000 type III secretion effector genes reveal functional overlap among effectors. *PLoS Pathogens*, 5, e1000388.

Landry, D., Gonzalez-Fuente, M., Deslandes, L. & Peeters, N. (2020) The large, diverse, and robust arsenal of *Ralstonia solanacearum* type III effectors and their in planta functions. *Molecular Plant Pathology*, 21, 1377–1388.

Le Roux, C., Huet, G., Jauneau, A., Camborde, L., Trémousaygue, D., Kraut, A. et al. (2015) A receptor pair with an integrated decoy converts pathogen disabling of transcription factors to immunity. *Cell*, 161, 1074–1088.

Lu, H., Lema, A.S., Planas-Marques, M., Alonso-Diaz, A., Valls, M. & Coll, N.S. (2018) Type III secretion-dependent and -independent

phenotypes caused by *Ralstonia solanacearum* in *Arabidopsis* roots. *Molecular Plant-Microbe Interactions*, 31, 175–184.

Mansfield, J., Genin, S., Magori, S., Citovsky, V., Sriariyanum, M., Ronald, P. et al. (2012) Top 10 plant pathogenic bacteria in molecular plant pathology. *Molecular Plant Pathology*, 13, 614–629.

Mukaihara, T., Hatanaka, T., Nakano, M. & Oda, K. (2016) *Ralstonia solanacearum* type III effector RipAY is a glutathione-degrading enzyme that is activated by plant cytosolic thioredoxins and suppresses plant immunity. *mBio*, 7, e00359–e416.

Nakano, M. & Mukaihara, T. (2019a) Comprehensive identification of PTI suppressors in type III effector repertoire reveals that *Ralstonia solanacearum* activates jasmonate signaling at two different steps. *International Journal of Molecular Sciences*, 20, 5992.

Nakano, M. & Mukaihara, T. (2019b) The type III effector RipB from *Ralstonia solanacearum* RS1000 acts as a major avirulence factor in *Nicotiana benthamiana* and other *Nicotiana* species. *Molecular Plant Pathology*, 20, 1237–1251.

Nakano, M., Oda, K. & Mukaihara, T. (2017) *Ralstonia solanacearum* novel E3 ubiquitin ligase (NEL) effectors RipAW and RipAR suppress pattern-triggered immunity in plants. *Microbiology*, 163, 992–1002.

Planas-Marquès, M., Kressin, J.P., Kashyap, A., Panthee, D.R., Louws, F.J., Coll, N.S. et al. (2020) Four bottlenecks restrict colonization and invasion by the pathogen *Ralstonia solanacearum* in resistant tomato. *Journal of Experimental Botany*, 71, 2157–2171.

Popa, C., Li, L., Gil, S., Tatjer, L., Hashii, K., Tabuchi, M. et al. (2016) The effector AWR5 from the plant pathogen *Ralstonia solanacearum* is an inhibitor of the TOR signalling pathway. *Scientific Reports*, 6, 27058.

Poueymiro, M., Cazale, A.C., Francois, J.M., Parrou, J.L., Peeters, N. & Genin, S. (2014) A *Ralstonia solanacearum* type III effector directs the production of the plant signal metabolite trehalose-6-phosphate. *mBio*, 5, e02065-14.

Poueymiro, M., Cunnac, S., Barberis, P., Deslandes, L., Peeters, N., Cazale-Noel, A.C. et al. (2009) Two type III secretion system effectors from *Ralstonia solanacearum* GMI1000 determine host-range specificity on tobacco. *Molecular Plant-Microbe Interactions*, 22, 538–550.

Quezada, C.M., Hicks, S.W., Galan, J.E. & Stebbins, C.E. (2009) A family of *Salmonella* virulence factors functions as a distinct class of autoregulated E3 ubiquitin ligases. *Proceedings of the National Academy of Sciences USA*, 106, 4864–4869.

Sabbagh, C.R.R., Carrere, S., Lonjon, F., Vailleau, F., Macho, A.P., Genin, S. et al. (2019) Pangenomic type III effector database of the plant pathogenic *Ralstonia* spp. *Peer J*, 7, e7346.

Sang, Y., Wang, Y., Ni, H., Cazale, A.C., She, Y.M., Peeters, N. et al. (2018) The *Ralstonia solanacearum* type III effector RipAY targets plant redox regulators to suppress immune responses. *Molecular Plant Pathology*, 19, 129–142.

Sang, Y., Yu, W., Zhuang, H., Wei, Y., Derevnina, L., Yu, G. et al. (2020) Intra-strain elicitation and suppression of plant immunity by *Ralstonia solanacearum* type-III effectors in *Nicotiana benthamiana*. *Plant Communications*, 1, 100025.

Sarris, P., Duxbury, Z., Huh, S., Ma, Y., Segonzac, C., Sklenar, J. et al. (2015) A plant immune receptor detects pathogen effectors that target WRKY transcription factors. *Cell*, 161, 1089–1100.

Senthil-Kumar, M., Hema, R., Anand, A., Kang, L., Udayakumar, M. & Mysore, K.S. (2007) A systematic study to determine the extent of gene silencing in *Nicotiana benthamiana* and other Solanaceae species when heterologous gene sequences are used for virus-induced gene silencing. *New Phytologist*, 176, 782–791.

Singer, A.U., Rohde, J.R., Lam, R., Skarina, T., Kagan, O., DiLeo, R. et al. (2008) Structure of the *Shigella* T3SS effector IpaH defines a new class of E3 ubiquitin ligases. *Nature Structural & Molecular Biology*, 15, 1293–1301.

Singer, A.U., Schulze, S., Skarina, T., Xu, X., Cui, H., Eschen-Lippold, L. et al. (2013) A pathogen type III effector with a novel E3 ubiquitin ligase architecture. *PLoS Pathogens*, 9, e1003121.

Sole, M., Popa, C., Mith, O., Sohn, K.H., Jones, J.D., Deslandes, L. et al. (2012) The *awr* gene family encodes a novel class of *Ralstonia solanacearum* type III effectors displaying virulence and avirulence activities. *Molecular Plant-Microbe Interactions*, 25, 941–953.

Spallek, T., Robatzek, S. & Gohre, V. (2009) How microbes utilize host ubiquitination. *Cellular Microbiology*, 11, 1425–1434.

Sun, T., Wu, W., Wu, H., Rou, W., Zhou, Y., Zhuo, T. et al. (2020) *Ralstonia solanacearum* elicitor RipX induces defense reaction by suppressing the mitochondrial *atpA* gene in host plant. *International Journal of Molecular Sciences*, 21, 2000.

Sun, Y., Li, P., Deng, M., Shen, D., Dai, G., Yao, N. et al. (2017) The *Ralstonia solanacearum* effector RipAK suppresses plant hypersensitive response by inhibiting the activity of host catalases. *Cellular Microbiology*, 19, e12736.

Szczesny, R., Buttner, D., Escolar, L., Schulze, S., Seiferth, A. & Bonas, U. (2010) Suppression of the AvrBs1-specific hypersensitive response by the YopJ effector homolog AvrBsT from *Xanthomonas* depends on a SNF1-related kinase. *New Phytologist*, 187, 1058–1074.

Valls, M., Genin, S. & Boucher, C. (2006) Integrated regulation of the type III secretion system and other virulence determinants in *Ralstonia solanacearum*. *PLoS Pathogens*, 2, e82.

Wan, W.L., Frohlich, K., Pruitt, R.N., Nurnberger, T. & Zhang, L. (2019) Plant cell surface immune receptor complex signaling. *Current Opinion in Plant Biology*, 50, 18–28.

Wang, H., Hu, J., Lu, Y., Zhang, M., Qin, N., Zhang, R. et al. (2019) A quick and efficient hydroponic potato infection method for evaluating potato resistance and *Ralstonia solanacearum* virulence. *Plant Methods*, 15, 145.

Wang, Y., Zhao, A., Morcillo, R.J.L., Yu, G., Xue, H., Rufian, J.S. et al. (2021) A bacterial effector protein uncovers a plant metabolic pathway involved in tolerance to bacterial wilt disease. *Molecular Plant*, 14, 1281–1296.

Wu, D., von Roepenack-Lahaye, E., Buntru, M., de Lange, O., Schandry, N., Pérez-Quintero, A.L. et al. (2019) A plant pathogen type III effector protein subverts translational regulation to boost host polyamine levels. *Cell Host & Microbe*, 26, 638–649 e635.

Xian, L., Yu, G., Wei, Y., Rufian, J.S., Li, Y., Zhuang, H. et al. (2020) A bacterial effector protein hijacks plant metabolism to support pathogen nutrition. *Cell Host & Microbe*, 28, 548–557 e547.

Xin, D.-W., Liao, S., Xie, Z.-P., Hann, D.R., Steinle, L., Boller, T. et al. (2012) Functional analysis of NopM, a novel E3 ubiquitin ligase (NEL) domain effector of *Rhizobium* sp. strain NGR234. *PLoS Pathogens*, 8, e1002707.

Yu, G., Xian, L., Xue, H., Yu, W., Rufian, J.S., Sang, Y. et al. (2020) A bacterial effector protein prevents MAPK-mediated phosphorylation of SGT1 to suppress plant immunity. *PLoS Pathogens*, 16, e1008933.

Zheng, N. & Shabek, N. (2017) Ubiquitin ligases: structure, function, and regulation. *Annual Review of Biochemistry*, 86, 129–157.

Zheng, X., Li, X., Wang, B., Cheng, D., Li, Y., Li, W. et al. (2019) A systematic screen of conserved *Ralstonia solanacearum* effectors reveals the role of RipAB, a nuclear-localized effector that suppresses immune responses in potato. *Molecular Plant Pathology*, 20, 547–561.

Zhou, J.M. & Zhang, Y. (2020) Plant immunity: danger perception and signaling. *Cell*, 181, 971–989.

Zhu, Y., Li, H., Hu, L., Wang, J., Zhou, Y., Pang, Z. et al. (2008) Structure of a *Shigella* effector reveals a new class of ubiquitin ligases. *Nature Structural & Molecular Biology*, 15, 1302–1308.

Zhuo, T., Wang, X., Chen, Z., Cui, H., Zeng, Y., Chen, Y. et al. (2020) The *Ralstonia solanacearum* effector RipI induces a defence reaction by

interacting with the bHLH93 transcription factor in *Nicotiana benthamiana*. *Molecular Plant Pathology*, 21, 999–1004.

SUPPORTING INFORMATION

Additional supporting information may be found in the online version of the article at the publisher's website.

How to cite this article: Niu, Y., Fu, S., Chen, G., Wang, H., Wang, Y., Hu, J., et al (2022) Different epitopes of *Ralstonia solanacearum* effector RipAW are recognized by two *Nicotiana* species and trigger immune responses. *Molecular Plant Pathology*, 23, 188–203. https://doi.org/10.1111/mpp.13153